Synthesis, biological activity and solution structure of new analogues of the antimicrobial Gramicidin S

Elżbieta Kamysz,[a]* Beata Mickiewicz,[a] Wojciech Kamysz,[b] Sylwia Bielińska,[b] Sylwia Rodziewicz-Motowidło[a] and Jerzy Ciarkowski[a]

Gramicidin S (GS) is a cyclo-decapeptide antibiotic isolated from *Bacillus brevis*. The structural studies have shown that GS forms a two-stranded antiparallel β-sheet imposed by two II' β-turns. Despite its wide Gram+ and Gram− antimicrobial spectrum, GS is useless in therapy because of its high hemotoxicity in humans. It was found, however, that the analogues of GS-14 (GS with 14 amino acid residues) attained a better antimicrobial selectivity when their amphipatic moments were perturbed. In this study, we report effects of similar perturbations imposed on GS cyclo-decapeptide analogues. Having solved their structures by NMR/molecular dynamics and having tested their activities/selectivities, we have concluded that the idea of perturbation of the amphipatic moment does not work for GS-10_0 analogues. An innovative approach to the synthesis of head-to-tail cyclopeptides was used. Copyright © 2010 European Peptide Society and John Wiley & Sons, Ltd.

Supporting information may be found in the online version of this article

Keywords: antimicrobial peptide; gramicidin S; amphipathicity; cyclic peptide synthesis; NMR; molecular dynamics; hemolysis; structure-activity relationship

Introduction

Gramicidin S (GS, *Gramicidin Soviet*) is a peptide antibiotic, cyclo-(Val-Orn-Leu-D-Phe-Pro)$_2$, isolated from *Bacillus brevis,* a gram-positive aerobic bacteria [1]. The structural studies confirmed that GS forms a two-stranded antiparallel β-sheet imposed by two II' β-turns [2,3] with the -D-Phe-Pro- pairs at the corners. GS forms a characteristic amphipathic structure, which displays a hydrophobic face, formed by Val and Leu residues on the one side of cyclic chain, and on the other side a second polar face formed by Orn side chains. The stabilization of the peptide structure is ensured by four regular backbone–backbone hydrogen bonds: two pairs of bonds between NH(Leu)–O(Val) and NH(Val)–O(Leu) [2]. It was found that the distribution of hydrophobic and hydrophilic residues on the opposite sides of the β-sheet is a structural feature required for the antimicrobial activity of GS [4]. Despite its wide gram-positive and gram-negative antimicrobial spectrum, GS is useless in therapy because of its high hemotoxicity in humans [5]. However, it was found that the analogues with D-His and Lys residues in place of the D-Phe and Orn ones were characterized by a good biological activity and reduced hemotoxicity [5,6]. Based on the studies of GS analogues with 14 amino acid residues (GS-14, Lys-Leu inserted into each strand), it was found that if their amphipathic moments were perturbed either by swap of adjacent Lys↔Leu/Val or by configuration reversal at Lys, the peptides acquired enhanced antimicrobial selectivity and suppressed hemotoxicity [7]. In this study, we report on the effects of similar perturbations imposed on GS original cyclo-decapeptide through testing the following examples: cyclo-(Val-Lys-Leu-D-His-Pro)$_2$, labeled GS10_0, [6] as the parent compound, and its three analogues: GS10_1, cyclo-(Val-Leu-Lys-D-His-Pro-Val-Lys-Leu-D-His-Pro), having Lys^2-Leu^3 swapped; GS10_2, cyclo-(Lys-Val-Leu-D-His-Pro-Val-Lys-Leu-D-His-Pro), hav-

ing Val^1-Lys^2 swapped and GS10_3, cyclo-(Val-D-Lys-Leu-D-His-Pro-Val-Lys-Leu-D-His-Pro), with Lys^2 converted to D-configuration. This paper presents the synthesis and structure activity studies for four GS analogues (refer the sequences in Figure 1) using 2D-NMR spectroscopy and MD. The results of these investigations are compared with the published structural information about GS and other analogues in an attempt to understand which structural features are responsible for the high biological activity and low hemotoxicity of these peptides.

Classical approaches to the synthesis of a head-to-tail cyclic peptide involve preparation of the partially protected linear precursor by solution or solid-phase approaches, followed by cyclization in solution under high dilution conditions [8–11]. An appropriate resin for the synthesis of protected linear precursors is a 2-chlorotrityl chloride resin developed by Barlos [12]. The cleavage of the product from the 2-chlorotrityl chloride resin is performed under very mild conditions. The cleavage is performed using acetic acid (AcOH)/TFE/DCM [12–14] or 1–5% TFA in DCM containing 5% triisopropylsilane (TIS) [15]. The literature methods require the presence of an environmentally unfriendly solvent such as DCM. For this reason an attempt has been made in this work to overcome this problem.

* Correspondence to: Elżbieta Kamysz, University of Gdańsk, Faculty of Chemistry, Sobieskiego 18, Gdańsk, 80-952, Poland. E-mail: kamysz@chem.univ.gda.pl

a University of Gdańsk, Faculty of Chemistry, Sobieskiego 18, Gdańsk, 80-952, Poland

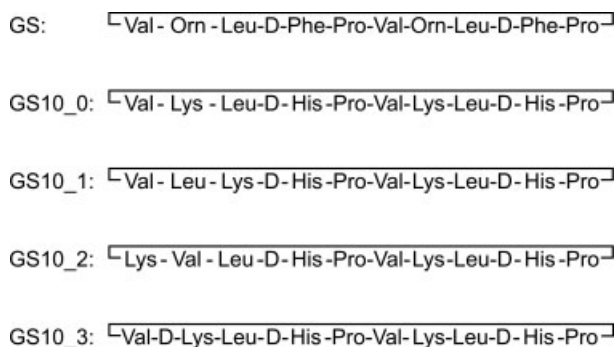b Medical University of Gdańsk, Faculty of Pharmacy, Al. Gen. J. Hallera 107, Gdańsk, 80-416, Poland

GS: Val - Orn - Leu-D-Phe-Pro-Val-Orn-Leu-D-Phe-Pro

GS10_0: Val - Lys - Leu-D-His-Pro-Val-Lys-Leu-D-His-Pro

GS10_1: Val - Leu - Lys-D-His-Pro-Val-Lys-Leu-D-His-Pro

GS10_2: Lys - Val - Leu-D-His-Pro-Val-Lys-Leu-D-His-Pro

GS10_3: Val-D-Lys-Leu-D-His-Pro-Val-Lys-Leu-D-His-Pro

Figure 1. Amino acid sequences of GS and its four analogues (GS10_0, GS10_1, GS10_2 and GS10_3).
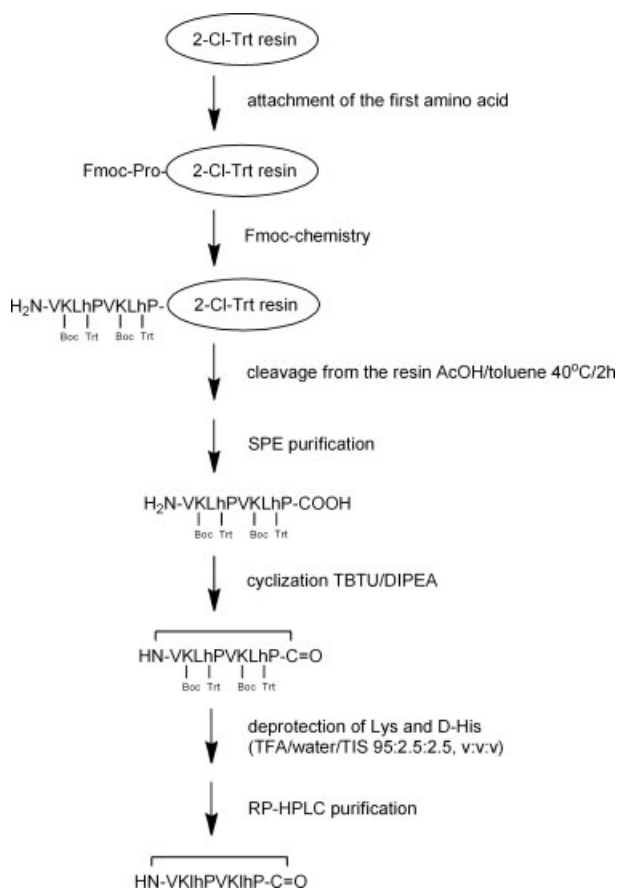

Figure 2. Scheme of the synthesis of cyclic GS analogues based on GS10_0 as an example.

Materials and Methods

Peptide Synthesis

Four analogues of GS were synthesized according to the scheme in Figure 2. First, linear peptides were synthesized manually by the solid-phase method on a 2-chlorotrityl chloride resin (substitution of Cl 1.3 mmol/g, 1% DVB, 100–200 mesh, Tianjin Nankai Hecheng Science & Technology Co., Ltd., China) using Fmoc chemistry [16]. N-α-Fmoc-protected amino acids were purchased from Iris Biotech GmbH (Germany); HOBt, piperidine, DIC and chloranil were from Fluka (Switzerland); DIEA, TIS and O-(benzotriazol-1-yl)-1,1,3,3-tetramethyluronium tetrafluoroborate (TBTU) were from

Sigma-Aldrich (Poland); acetonitrile, DMF, DCM, diethyl ether, AcOH and toluene were from Polish Chemicals (Poland).

The N-α-Fmoc-amino acids were protected on the side chain as follows:

Boc for lysine, Trt for His. The attachment of the first amino acid to the resin was performed according to Barlos *et al.* with a loading of 0.6 mmol/g [12]. Deprotection of the Fmoc group was carried out for 5 and 20 min with 25% piperidine in DMF. The coupling reactions were carried out with the protected amino acid (Fmoc-AA) dissolved in DMF/DCM using HOBt and DIC for 2 h (Fmoc-AA : HOBt : DIC, 1 : 1 : 1). The completeness of each coupling step was monitored by the chloranil test. If positive, the coupling reactions were repeated using TBTU with addition of HOBt in the presence of DIEA for 2 h (Fmoc-AA : TBTU : HOBt : DIEA, 1 : 1 : 1 : 2).

After the synthesis has been completed, the peptide resins were dried under vacuum. The peptides were cleaved from the resins using a 50% AcOH/toluene mixture at 40 °C three times (3 × 2 h). Under these conditions, the cleaved peptides were protected in their side chain functions. The resins were filtered off and the solutions were evaporated under reduced pressure. The peptides were precipitated from cold water, centrifuged and lyophilized. The yields of the protected linear peptides after the cleavage from the resin were 79–86, 13–18 and 1–3% after the first 2 h, the next 2 h, and the last 2 h, respectively. The HPLC purity of peptides after the cleavage from the resin was higher than 90%. The peptides were purified using solid-phase extraction (SPE) as described in our previous work [17].

In the next step, the cyclization was performed. To a solution of 0.1 mmol of the peptide in 300 ml of DMF, a solution of TBTU/DIPEA (molar ratio 1 : 2) in DMF was added. The progress of the reaction was monitored by HPLC. After the cyclization has been completed, the protecting groups on the side chains were removed using a TFA/water/TIS (95 : 2.5 : 2.5, v : v : v) mixture. Purification was performed using the RP-HPLC on a Kromasil C8 column (8 × 250 mm, 5 µm particle size) with several linear gradients of acetonitrile (ACN) in 0.1% TFA. The eluates were fractionated and analyzed by the analytical RP-HPLC. The purity of the peptides was checked on an analytical Beckman Gold chromatograph with a Kromasil C8 column (4.6 × 250 mm, 5 µm particle size) or on a Varian ProStar HPLC system controlled by Galaxie Chromatography Data System with Phenomenex Luna C18 column (4.6 × 150 mm, 3 µm particle size) with several linear gradients of ACN in 0.1% TFA. Fractions containing the pure peptides (>98%) were pooled and lyophilized. The peptides were subsequently analyzed by MALDI-TOF MS. The values of the molecular ions were as expected.

Antimicrobial Susceptibility Testing

MIC was determined by the microbroth dilution method outlined by the National Committee for Clinical and Laboratory Standards (NCCLS). The following control strains were tested: gram-positive: *Bacillus subtilis* ATCC 9372, *Enterococcus faecalis* ATCC 29212, *Rhodococcus equi* ATCC 6939, *Staphylococcus aureus* ATCC 6538 and *Staphylococcus epidermidis* ATCC 14990; gram-negative: *Escherichia coli* ATCC 8739, *Klebsiella pneumoniae* ATCC 700603, *Proteus vulgaris* ATCC 6038 and *Candida albicans* ATCC 10231 strain as a representative of fungi. All the microorganisms were obtained from the Polish Collection of Microorganism (Polish Academy of Science, Wroclaw, Poland). As culture media, Mueller–Hinton broth was used for bacteria and Sabouraud glucose broth for *Candida albicans*. Microbial cells were exposed to the cyclic

peptides at adequate concentrations (range: 64–2000 µg/ml) for 18 h at 37 °C (bacterial strains) or 18 h at 25 °C (*C. albicans*).

Hemolysis Assay

Fresh human blood was collected into tubes containing EDTA as anticoagulant. Red blood cells were separated by centrifugation at 500 × g for 12 min at room temperature and the plasma was aspirated. Erythrocytes were washed three times with PBS, separated by centrifugation (500 × g, 12 min) and resuspended in PBS. The cyclic peptides (GS10_1, GS10_2 and GS10_3) were serially diluted in PBS (range 1–2000 µg/ml) and 50 µl was added to 50 µl of the erythrocyte suspension. The final concentration of red blood cells was 4% [v/v]. The results were assessed visually after the incubation for 1 h at 37 °C. As a positive control, 1% Triton was used, whereas PBS served as a negative control.

NMR Experiments

The NMR samples were prepared by dissolving the peptides in a D_2O/H_2O (10/90% by volume). Sample concentrations were 3 mM. Chemical shifts are given relative to 4,4-dimethyl-4-silapentane-1-sulfonic acid (DSS), the internal chemical shift standard. ^{1}H-NMR NMR spectra (Varian Unity) were obtained at a frequency of 500 MHz at 22, 32, 40 and 50 °C. 2D spectra, including DQF-COSY, TOCSY (80 ms), NOESY (100 ms), ROESY (200 ms) and ^{1}H-^{13}C HSQC, were recorded at 32 °C. The NMR data were processed with VNMR [18] and analyzed with a XEASY software [19]. Assignments were carried out according to standard procedures, including spin-system identification and sequential assignment [20]. $^3J_{NH-\alpha H}$ vicinal coupling constants were determined by 2D DQF-COSY experiments. Distance constraints and coupling constants were used in the HABAS program [21] of the DYANA package [22] to generate Φ, ψ and χ^1 dihedral angle constraints and stereospecific assignments. Dihedral angle constraints were calculated from the Karplus equation with A = 6.4, B = −1.4 and C = 1.9 [23].

Intensities of rotating nuclear Overhauser effect (ROE) were determined from the ROESY (200 ms) spectra of the GS analogues. ROE volumes were integrated and calibrated with the XEASY software [19]. After internal calibration, the cross-peaks from the ROESY experiments were converted into upper distance limits with the CALIBA program of the DYANA package [22]. Based on the experimental chemical shifts of the αC amino acid residues, chemical shift indexes (CSI) were calculated relative to the DSS reference 24.

Structure Calculations

Structures of the peptides were determined by MD simulations with the time-averaged restraint methodology (TAV) [25–27], which were carried out with the AMBER force field [28] using the AMBER 8.0 package [27]. In MD calculations, the interproton distances and dihedral angles were used as time-restrained restraints. The interproton distances were restrained with the force constant k = 20 kcal/(mol × Å^2) and the dihedral angles with k = 2 kcal/(mol × rad^2), respectively. The dihedral angles ω were restrained with a center at 180° and k = 10 kcal/(mol × rad^2). The improper dihedral angles centered at the αC atoms (defining the chirality of amino acid residues) were restrained with k = 50 kcal/(mol × rad^2). All simulations were carried out in a TIP3P [29] periodic water box at constant volume using the particle-mesh Ewald procedure for long-range electrostatic interactions

Table 1. Physicochemical properties of cyclopeptides GS10_0–GS10_3

Peptide	Formula	HPLC R_t(min)[a]	[M + H]$^+$ found (calculated)
GS10_0	$C_{56}H_{92}N_{16}O_{10}$	14.3	1149.4 (1149.7)
GS10_1	$C_{56}H_{92}N_{16}O_{10}$	14.4	1149.4 (1149.7)
GS10_2	$C_{56}H_{92}N_{16}O_{10}$	13.9	1149.5 (1149.7)
GS10_3	$C_{56}H_{92}N_{16}O_{10}$	14.4	1149.2 (1149.7)

RP-HPLC analytical analyses were performed on a Varian ProStar HPLC system equipped with Galaxie Chromatography Data System.
[a] Linear gradient from 3 to 60% of [B] for 30 min, Phenomenex Luna C18 column (3 µm, 150 × 4.6 mm) using a flow rate of 1 ml/min and with the following solvent systems: 0.1% aqueous TFA [A], 0.1% TFA in acetonitrile [B].

[30]. MD simulations, with time-averaged restraints, were run at 300 K and a time step of 2 fs. The total duration of the run was 4200 ps. From every trajectory, a final set of 200 last conformations was collected for analysis. All sets of conformations were clustered separately with the use of the MOLMOL program [31]. A root mean square (RMS) deviation cut-off of 3.5 Å was used in the clustering procedure. The clustering procedure provided five families of conformations for each peptide (GS10_0, GS10_1, GS10_2 and GS10_3). The four most populated families were selected for presentation. The RMS deviation was calculated based on αC atoms. The graphic MOLMOL program was also used to display the electrostatic potential on the van der Waals surface of the peptides.

Results and Discussion

Peptide Synthesis

We have developed a simple method for chemical synthesis of His containing head-to-tail cyclopeptides based on the standard solid-phase method using Fmoc chemistry. Using our method we have synthesized four cyclic analogues of GS. Their physicochemical data are presented in Table 1. The warm solution of AcOH in toluene used in this method for removing the protected peptides from the resin can readily be removed after completing the reaction, and it is more environmentally friendly than the commonly used solution of TFA in DCM. Previously, the head-to-tail His-containing cyclopeptides were synthesized by the solid-phase methodology using Fmoc chemistry based on anchoring the imidazole ring of a His residue to the trityl-resin [32–34]. In the case of cyclopeptides that did not include the His residue, the synthesis was performed by the solid-phase methodology using Boc chemistry [35]. Our innovative approach seems to be more universal because it can be applied to the preparation of cyclopeptides with and without the His residue. Moreover, this method is so simple and robust that it can be used not only on the laboratory scale but can also be useful for upgrading the synthesis.

Antimicrobial and Hemolytic Activity

The biological activities of the synthesized peptides were tested against gram-positive bacteria, gram-negative bacteria and fungi. We have classified all the tested compounds as microbiologically inactive as they did not exhibit antimicrobial activity at the concentrations applied.

All the tested compounds showed low levels of hemolytic activity. The lysis of human red blood cells was observed only for the GS10_1 peptide at a concentration of 1000 µg/ml, whereas the remaining compounds did not exhibit the hemolytic activity at the applied concentrations.

Nuclear Magnetic Resonance

The 2D-NMR spectra of the peptides, obtained via the standard sequential assignment methods developed by Wüthrich [20], were interpreted (Figures S1 and S2 in Supporting Information). Using the TOCSY spectra (80 ms), the proton chemical shifts were recognized and using the ROESY spectra (200 ms), the sequences of four analogues were confirmed. In the 2D-NMR spectra of peptide GS10_0, there were only five spin systems because of a doubled pentapeptide sequence of this analogue. For GS10_0 and GS10_3, there were some signals indicative of two sets of conformations: a major and a minor one (GS10_0: 70% major and 30% minor conformation; GS10_3: 90% major and 10% minor conformation). For analogues GS10_0 and GS10_3, there were also additional signals for a particular amino acid residue, which indicated a high flexibility of these peptides in the solvent environment. The chemical shifts of the protons, $^3J_{NH-\alpha H}$ vicinal coupling constants and amide-proton temperature coefficients for the peptides are described in Tables SI–SIV (Supporting Information). Examination of the ROESY spectra revealed the *trans* geometry of all the peptide bonds in the analogues. There were no chemical exchange cross-peaks, which could indicate *cis/trans* isomerisation [36].

Additionally, the strong coupling values between the αH_i and NH_{i+1} protons confirmed the *trans* geometry for all the peptide bonds. In Figure 2, the ROE effects corresponding to interproton distances, CSI, $^3J_{NH-\alpha H}$ vicinal coupling constants and amide-proton temperature coefficients are presented. For peptides GS10_0 and GS10_3, only signals for major conformations were analyzed, because ROE connectivities for minor conformations were very weakly exposed.

The sequential $\alpha H_i - NH_{i+1}$ ROE connectivities are always seen in the recorded spectra and there are also some of $\beta H_i - NH_{i+1}$ ROEs. This indicates the presence of β-turns in the peptides' structures, but there are no diagnostic $NH_i - NH_{i+1}$ ROEs, thus revealing the lack of a regular β-sheet structure of the peptides [37]. The $\alpha H_i - NH_{i+1}$ and $\beta H_i - NH_{i+1}$ ROE connectivities for the Val1–Lys2 and Val6–Lys7 region of GS10_0 and for the Val1–Leu2 and Val6–Lys7 regions of GS10_1 as well as for the D-Lys2–Leu3, Val6–Lys7 and Lys7–Leu8 regions of GS10_3 suggest the formation of β-turns in these parts of the molecules (Figure 3).

The CSI, defined as the deviation of the random-coil chemical shift from the experimental value, is a sensitive indicator of the secondary structure of peptides and proteins [38]. Our results show that in the GS10_0 and GS10_1 peptides, most of the amino acids have CSI values characteristic of the β-sheet structure (CSI = −1). The CSIs for other analogues display no regularity, which indicates a predominantly random structure (Figure 3). Moreover, the large values of the $^3J_{NH-\alpha H}$ vicinal coupling constants (>8.5 Hz) in the
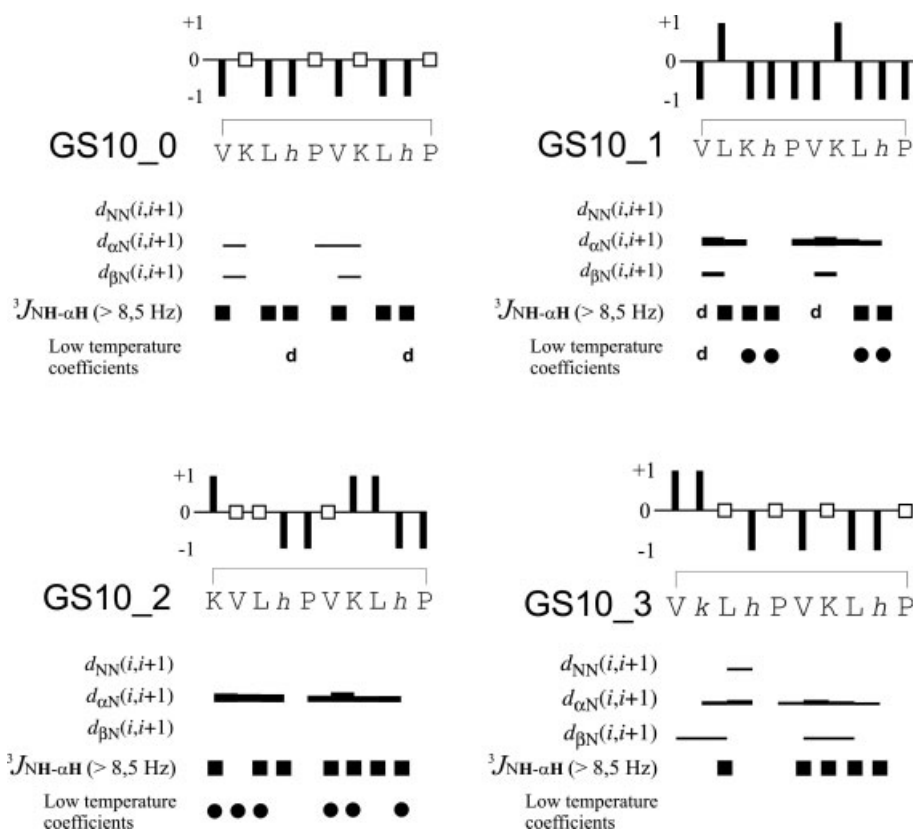

Figure 3. CSIs relative to DSS, summary of intra- and interresidual ROEs among the backbone NH, αH and βH, $^3J_{NH-\alpha H}$ vicinal coupling constants and temperature coefficients of amide protons for GS10_0 (major conformation), GS10_1, GS10_2 and GS10_3 (major conformation) measured in D$_2$O/H$_2$O (1:9, v/v) at 32 °C. CSIs equal to zero for amino acid residues are labeled with empty squares. Bar height indicates the strength of the ROE correlation as being strong, medium or weak. Solid squares show $^3J_{NH-\alpha H}$ coupling constants >8.5 Hz, and solid circles the low temperature coefficients of amide groups (<3.0). 'd' – difficult to measure.

sequences of the peptides suggest the presence of the β-sheet structure for these molecules [37] (Figure 3).

To detect hydrogen bonds, we used the data from 1D ^{1}H-NMR spectra recorded at different temperatures to calculate the temperature coefficients for all the amide protons in the peptides (Figure 3 and Tables SI–SIV). Very low values of the temperature coefficients (below -3.0×10^{-3} ppm/K) indicate the absence of stable hydrogen bonds and a regular structure of the peptides [39]. The temperature coefficients for the GS10_0 and GS10_3 peptides are lower than -3.0×10^{-3} ppm/K, thus suggesting that the peptides do not have stable hydrogen bonds. However, the diagnostic data mentioned above (CSI, coupling constant) for the GS10_0 peptide suggest the presence of the β-sheet structure for this molecule. Most probably the low values of the temperature coefficients for GS10_0 results from the high flexibility of the peptide in the solvent environment (the presence of two sets of conformations: a major and a minor one). Regarding GS10_1, only one amino acid residue, Val 6 (the temperature coefficients

lower than -5.0×10^{-3} ppm/K) is not involved in hydrogen bond formation. The remaining amino acid residues in GS10_1 form hydrogen bonds which stabilize the peptide structure. With GS10_2 almost all the amino acid residues form strong hydrogen bonds stabilizing the peptide structure. This indicates that the rings of these peptides are quite stable and inflexible in the solvent environment, this in turn, confirming the absence of sets of conformations in contrast to those in the GS10_0 and GS10_3 peptides.

Structural Analysis

Conformational analyses were performed for four GS (GS10) analogues in an attempt to correlate their structure with their activity in comparison with native GS10. Structures of peptides GS10_0 (major conformation), GS10_1, GS10_2 and GS10_3 (major conformation) were determined by MD simulations with the TAV. For each GS analogue, 200 conformations were obtained and
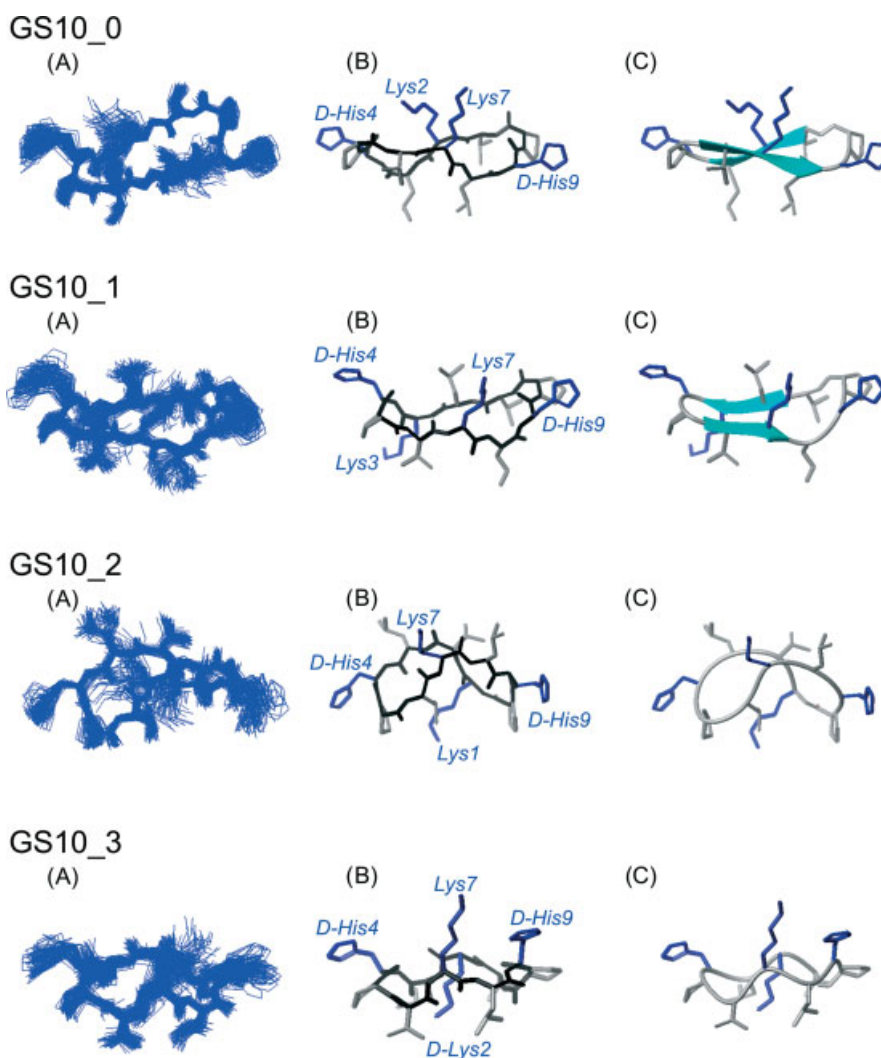

Figure 4. Most populated families of conformations of GS analogues: GS10_0 (major conformation), GS10_1, GS10_2 and GS10_3 (major conformation) obtained by using time-averaged MD methodology with restraints from NMR measurements. Left column (A) shows all conformations of the family (only backbones and side chains without hydrogen atoms are shown for clarity); (B) the lowest-energy conformation from the corresponding family (all heavy atoms are shown, the backbone is shown in black color, Lys and D-His residues in blue, other amino acid residues in gray); (C) the lowest-energy conformation from the corresponding family in ribbon presentation (all heavy atoms are shown). A total of 800 conformations were subjected to a cluster analysis, leading to the following numbers and percentages of each clustered family: GS10_0, 128 (64%); GS10_1, 91 (46%); GS10_2, 72 (36%) and GS10_3, 74 (37%).

the RMSD values of the αC atoms of all residues were GS10_0 = 0.41 Å, GS10_1 = 0.46 Å, GS10_2 = 0.35 Å and GS10_3 = 0.43 Å. All conformations were subjected to a cluster analysis, leading to the following numbers of most populated clustered families: GS10_0, 128 conformations; GS10_1, 91 conformations; GS10_2, 72 conformations and GS10_3, 74 conformations.

Our conformational studies show that GS10_0 forms a two-stranded antiparallel β-sheet imposed by two II′ β-turns with the -D-His-Pro- pairs at the corners (Figure 4). A very similar structure but with a shorter β-sheet is formed by the GS10_1 peptide (Figure 4). The other analogues, GS10_2 and GS10_3, do not form a regular β-hairpin structure (Figure 4). The β-sheet structure of GS10_0 is strongly stabilized by three regular backbone–backbone hydrogen bonds: NH(Leu3)–O(Val6), NH(Leu8)–O(Val1) and NH(Val1)–O(Leu8). In turn, a shorter β-sheet structure GS10_1 is stabilized by two backbone–backbone hydrogen bonds: NH(Lys3)–O(Val6) and NH(Leu8)–O(Val1).

Despite the differences between conformations of the four GS analogues, the structures of all peptides are characterized by amphiphilicity. This means that the cationic and non-polar sides could be distinguished in the structures (Figure 4). The polar side is built by Lys and D-His residues and the hydrophobic face is formed by other amino acid residues. However, only in the GS10_0 peptide are the side chains of Lys and D-His residues located on the same side of the ring to form a big bulky polar region on the one side and the non-polar region on the other side of the peptide structure (Figure 4). In the other analogues (GS10_1, GS10_2 and GS10_3), the side chains of the Lys residues are located on the opposite sides of the cyclic rings (Figure 4), and therefore the electrostatic potential is not located symmetrically against the surface of the cyclic rings. In consequence, the presence of the cationic side chains of Lys residues in the non-polar regions of the peptides reduces the hydrophobic moment of the molecules and is likely to affect the mode of action of the GS analogues.

Conclusion

GS is active against gram-positive and gram-negative bacteria and fungi [6]. The peptide is also extremely hemolytic against human erythrocytes that preclude its use in therapy [5]. Its analogue, GS10_0, shows hemolytic activity against human red blood cells while exhibiting antibacterial activity [6]. To be useful as an antibiotic, it would be desirable for the analogues to exhibit antimicrobial activity with a low hemolytic activity. The literature on the GS derivatives shows that effective separation of antimicrobial activity and hemotoxicity could only be achieved when the amphipathic moments of a reference compound are perturbed [7]. In this study, we have found that similar perturbations imposed on the GS10_0 analogue did not work. Although all the studied analogues are characterized by low hemotoxicity, drastically reduced microbiological activity has also been noticed. The perturbation of amphipathic moments in the studied molecules causes destabilization of the secondary structure of the peptides, thus dramatically reducing their antimicrobial activity. Summing up, the presence of the β-sheet structure with relevant distribution of hydrophobic and hydrophilic potentials on the β-sheet surface is the key feature for maintaining the high biological activity and low hemolytic activity of the GS analogues. However, studies on a larger number of such designed peptides will certainly augment our understanding of the role of the distribution of hydrophobic and hydrophilic residues

on the opposite sides of the β-sheet and the consequence of their influence on peptide conformation. Nevertheless, the conclusions reached in the present study can be useful for the design of the new GS analogues with a better pharmacological profile. The results indicate that a better understanding of structural features responsible for the mode of action of these peptides is crucial for the development of a new generation of antibiotics.

The synthesis of the GS analogues demonstrated feasibility of our innovative approach in synthesizing head-to-tail cyclopeptides with His residue. The method is compatible with Fmoc-chemistry and can also be applicable to the synthesis of cyclic peptides without the His residue. To the best of our knowledge, for the first time the protected precursors for the synthesis of head-to-tail cyclopeptides were cleaved from the 2-chlorotrityl chloride resin without using the environmentally-unfriendly solvent such as DCM. It is the simple and robust method that can be used not only on the laboratory scale but is also likely to be applicable on a large scale.

Supporting information

Supporting information may be found in the online version of this article.

References

1 Gause GF, Brazhnikova MG. Gramicidin S and its use in the treatment of infected wounds. *Nature* 1944; **154**: 703.
2 Stern A, Gibbons WA, Craig LC. A Conformational analysis of gramicidin S-A by nuclear magnetic resonance. *Proc. Natl. Acad. Sci. U. S. A.* 1968; **61**: 734–741.
3 Rackovsky S, Scheraga HA. Intermolecular anti-parallel β sheet: comparison of predicted and observed conformations of gramicidin S. *Proc. Natl. Acad. Sci. U. S. A.* 1980; **77**: 6965–6967.
4 Izumiya N, Kato T, Aoyaga H, Waki M, Kondo M. *Synthetic Aspects of Biologically Active Cyclic Peptides: Gramicidin S and Tyrocidines*. Halsted Press: New York, 1979; 49–89.
5 Kondejewski LH, Farmer SW, Wishart DS, Kay CM, Hancock REW, Hodges RS. Modulation of structure and antibacterial and hemolytic activity by ring size in cyclic gramicidin S analogs. *J. Biol. Chem.* 1996; **271**: 25261–25268.
6 Kondejewski LH, Farmer SW, Wishart DS, Hancock REW, Hodges RS. Gramicidin S is active against both gram-positive and gram-negative bacteria. *Int. J. Pept. Protein Res.* 1996; **47**: 460–466.
7 Lee DL, Hodges RS. Structure-activity relationships of de novo designed cyclic antimicrobial peptides based on gramicidin S. *Biopolymers* 2003; **71**: 28–48.
8 Yun-hua Y, Xing-ming G, Mian L, Yan-chun T, Gui-ling Tian. Studies on the synthetic methodology of head to tail cyclization of linear peptides. *Lett. Pept. Sci.* 2003; **10**: 571–579.
9 Tang YC, Xie HB, Tian GL, Ye YH. Synthesis of cyclopentapeptides and cycloheptapeptides by DEPBT and the influence of some factors on cyclization. *J. Pept. Res.* 2002; **60**: 95–103.
10 Valero ML, Giralt E, Andreu D. A comparative study of cyclization strategies applied to the synthesis of head-to-tail cyclic analogs of a viral epitope. *J. Pept. Res.* 1999; **53**: 56–67.
11 Alcaro MC, Sabatino G, Uziel J, Chelli M, Ginanneschi M, Rovero P, Papini AM. On-resin head-to-tail cyclization of cyclotetrapeptides: optimization of crucial parameters. *J. Pept. Sci.* 2004; **10**(4): 218–228.

12 Barlos K, Chatzi O, Gatos D, Stavropoulos G. 2-Chlorotrityl chloride resin. Studies on anchoring of Fmoc-amino acids and peptide cleavage. *Int. J. Pept. Protein Res.* 1991; **37**: 513–520.

13 Barlos K, Gatos D, Kapolos S, Poulos C, Schäfer W, Yao WQ. Application of 2-chlorotrityl resin in solid phase synthesis of (Leu15)-gastrin I and unsulfated cholecystokinin octapeptide. Selective O-deprotection of tyrosine. *Int. J. Pept. Protein Res.* 1991; **38**(6): 555–561.

14 Bodi J, Suli-Vargha H, Ludanyi K, Vekey K, Orosz G. New strategy for the synthesis of large peptides as applied to the C-terminal cysteine-rich 41 amino acid fragment of the mouse agouti protein. *Tetrahedron Lett.* 1997; **38**: 3293–3296.

15 Barlos K, Gatos D, Hatzi O, Koch N, Koutsogianni S. Synthesis of the very acid-sensitive Fmoc-Cys(Mmt)-OH and its application in solid-phase peptide synthesis. *Int. J. Pept. Protein Res.* 1996; **47**(3): 148–153.

16 Chan WC, White PD. *FMOC Solid Phase Peptide Synthesis. A Practical Approach*. Oxford University Press: Oxford, 2000.

17 Kamysz W, Okrój M, œempicka E, Ossowski T, œukasiak J. Fast and efficient purification of synthetic peptides by solid-phase extraction. *Acta Chromatogr.* 2004; **14**: 180–186.

18 Varian. *Nuclear Magnetic Resonance Instruments, VnmrTM Software.* Palo Alto, CA, 2002; Revision 5.3B 1/97.

19 Bartles C, Xia T, Billeter M, Güntert P, Wütrich K. The program XEASY for computer-supported NMR spectral analysis of biological macromolecules. *J. Biomol. NMR* 1995; **6**: 1–10.

20 Wüthrich K. *NMR of Proteins and Nucleic Acids*. Wiley Interscience: New York, 1986.

21 Güntert P, Braun W, Wüthrich K. Efficient computation of three-dimensional protein structures in solution from nuclear magnetic resonance data using the program DIANA and the supporting programs CALIBA, HABAS and GLOMSA. *J. Mol. Biol.* 1991; **217**: 517–530.

22 Güntert P, Wüthrich K. Improved efficiency of protein structure calculations from NMR data using the program DIANA with redundant dihedral angle constraints. *J. Biomol. NMR.* 1991; **1**: 447–456.

23 Karplus M. Contact Electron-Spin Coupling of Nuclear Magnetic Moments. *J. Phys. Chem.* 1959; **30**: 11–15.

24 Spera S, Bax A. Empirical correlation between protein backbone conformation and C and C ^{13}C nuclear magnetic resonance chemical shifts. *J. Am. Chem. Soc.* 1991; **113**: 5490–5492.

25 Torda AE, Scheek RM, van Gunsteren WF. Time-dependent distance restraints in molecular dynamics simulations. *Chem. Phys. Lett.* 1989; **157**: 289–294.

26 Pearlman DA, Kollman PA. Are time-averaged restraints necessary for nuclear magnetic resonance refinement? A model study for DNA. *J. Mol. Biol.* 1991; **220**: 457–479.

27 Case DA, Darden TA, Cheatham TE, *III*. Simmerling CL, Wang J, Duke RE, Luo R, Merz KM, Wang B, Pearlman DA, Crowley M, Brozell S, Tsui V, Gohlke H, Mongan J, Hornak V, Cui G, Beroza P, Schafmeister C, Caldwell JW, Ross WS, Kollman PA. *AMBER 8*. University of California: San Francisco, 2004.

28 Weiner SJ, Kollman PA, Nguyen DT, Case DA. An all atom forcefield for simulations of proteins and nucleic acid. *J. Comput. Chem.* 1986; **7**: 230–252.

29 Mahoney MW, Jorgensen WL. A five-site model liquid water and the reproduction of the density anomaly by rigid, non-polarizable models. *J. Chem. Phys.* 2000; **112**: 8910–8922.

30 Darden T, York D, Pedersen L. Particle Mesh Ewald-an N. Log(N) method for Ewald sums in large systems. *J. Chem. Phys.* 1993; **98**: 10089–10092.

31 Koradi R, Billeter M, Wütrich K. MOLMOL: a program for display and analysis of macromolecular structures. *J. Mol. Graph.* 1996; **14**(1): 51–55.

32 Sabatino G, Chelli M, Mazzucco S, Ginanneschi M, Papini AM. Cyclisation of histidine containing peptides in the solid-phase by anchoring the imidazole ring to trityl resins. *Tetrahedron Lett.* 1999; **40**: 809–812.

33 Brasuń J, Gabbiani Ch, Ginanneschi M, Messori L, Orfei M, Świątek-Kozłowska J. The copper(II) binding properties of the cyclic peptide c(HGHK). *J. Inorg. Biochem.* 2004; **98**: 2016–2021.

34 Malesevic M, Strijowski U, Bächle D, Sewald N. An improved method for the solution cyclization of peptides under pseudo-high dilution conditions. *J. Biotechnol.* 2004; **112**: 73–77.

35 Jelokhani-Niaraki M, Kondejewski LH, Wheaton LC, Hodges RS. Effect of ring size on conformation and biological activity of cyclic cationic antimicrobial peptides. *J. Med. Chem.* 2009; **52**: 2090–2097.

36 Dyson HJ, Rance M, Houghten RA, Lemer RA, Wright PE. Folding of immunogenic peptide fragments of proteins in water solution: I. Sequence requirements for the formation of a reverse turn. *J. Mol. Biol.* 1988; **201**: 161–200.

37 Evans JNS. *Biomolecular NMR Spectroscopy*. Oxford University Press: Oxford, 1995.

38 Wishart DS, Sykes BD, Richards FM. The chemical shift index: a fast and simple method for the assignment of protein secondary structure through NMR spectroscopy. *Biochemistry* 1992; **31**: 1647–1651.

39 Siemion IZ. *Biostereochemia*. Wydawnictwo Naukowe PWN: Warszawa, 1985.

217